NIH Public Access
Author Manuscript
Ultrasound Med Biol. Author manuscript; available in PMC 2015 February 01.

Published in final edited form as:
Ultrasound Med Biol. 2014 February ; 40(2): 351–360. doi:10.1016/j.ultrasmedbio.2013.09.026.

Evaluation of utero-placental and fetal hemodynamic parameters throughout gestation in pregnant mice using high-frequency ultrasound

Edgar Hernandez-Andrade[1,2], **Hyunyoung Ahn**[1,2], **Gabor Szalai**[1], **Steven J Korzeniewski**[1,2], **Bing Wang**[1], **Mary King**[1,2], **Tinnakorn Chaiworapongsa**[1,2], **Nandor Gabor Than**[1,2], and **Roberto Romero**[1]

[1]Perinatology Research Branch, NICHD/NIH/DHHS, Bethesda, MD, and Detroit, MI, USA

[2]Department of Obstetrics and Gynecology, Wayne State University School of Medicine, Detroit, Michigan, USA

Abstract

Changes throughout gestation of maternal and fetal Doppler parameters in pregnant mice, similar to those obtained in human fetuses, using a high frequency ultrasound with a 55 MHz linear probe are described. The uterine arteries (UtA), fetal umbilical (UA) and fetal ductus venosus (DV) showed: increased peak systolic velocity (UtA, p=0.04; UA, p=0.0004; DV, p=0.02), reduced end diastolic velocity (UtA, p<0.001; UA, p<.0001; DV, p=0.01), and reduced resistance index (UtA, p=0.0004; UA, p=0.0001; DV, p=0.04) toward the end of pregnancy. The middle cerebral (MCA) and carotid arteries (CAR) showed reduced end diastolic velocity (MCA, p=0.02; CAR, p<0.0001), and resistance index (both vessels, p<0.0001). The umbilical vein showed a reduction in the pulsatile pattern (p<0.05). Increased velocities and reduced resistance index suggest a progressive increment in blood flow to the fetal mouse towards the end of pregnancy. Evaluation of fetal and utero-placental vascular parameters in CD-1 mice can be reliably performed using high frequency ultrasound.

Keywords

Doppler; experimental mouse model; pregnancy; high frequency ultrasound

Introduction

Animal experimentation has been fundamental for describing the process of fetal cardiovascular development throughout pregnancy (Rudolph and Heymann 1968; Rudolph and Heymann 1970), and hemodynamic adaptation/deterioration when obstetric complications are present (Abi-Nader et al. 2012; Bennet et al. 1999; Berman et al. 1975; Bishai et al. 2003; Block et al. 1984; Rosen et al. 1986; Sheldon et al. 1979). Indeed, the

Address correspondence to: Roberto Romero, MD, D.Med.Sci., and Edgar Hernandez-Andrade, MD, PhD, Perinatology Research Branch, NICHD, NIH, DHHS, Wayne State University / Hutzel Women's Hospital, 3990 John R, Box 4, Detroit, Michigan, 48201 USA, Telephone: 313-993-2700, Fax: 313-993-2694, romeror@mail.nih.gov & ehernand@med.wayne.edu.

Declaration of Interest: The authors report no declarations of interest.

NIH-PA Author Manuscript
NIH-PA Author Manuscript
NIH-PA Author Manuscript

NIH-PA Author Manuscript

NIH-PA Author Manuscript

NIH-PA Author Manuscript

process of blood flow distribution in fetal organs was originally described in fetal sheep using radiolabeled microspheres (Heymann et al. 1977; Heymann and Rudolph 1967; Rudolph and Heymann 1967; Rudolph and Heymann 1972). Recently, other animal models have also been proposed; pregnant murine and rabbit models (Bassan et al. 2000; Eixarch et al. 2009; Eixarch et al. 2011) have shorter gestational periods requiring smaller experimental areas, relatively lower costs, higher number of fetuses, and have similar characteristics as the human placenta (Malassine et al. 2003; Sapin et al. 2001). The use of knock-out mouse strains provides further advantages in studying the effects of specific genes during pregnancy (Pham et al. 2009; Smith et al. 2007; Tian et al. 2006; Zhang et al. 2011).

Doppler ultrasound has proven value in assessing fetal and maternal cardiovascular parameters in animal experimentation (Acharya et al. 2008; Ferrazzi et al. 2001; Gudmundsson et al. 1990; Gunnarsson et al. 1998; Hernandez-Andrade et al. 2005; Schmidt et al. 1991). However, conventional Doppler ultrasound emitting at frequencies between 2 MHz and 16 MHz does not have the temporal resolution required to clearly display Doppler waveforms and color Doppler maps in murine models (such as the mouse) with a cardiac rate of 350–500 bpm (Stypmann 2007). High frequency ultrasound enables fast signal acquisition and processing by using linear probes emitting at 25–55 MHz (Phoon et al. 2000; Renault et al. 2006). The Doppler waveforms clearly display all velocity components, and the color Doppler mapping provides reliable information about the direction of the flow (Stypmann 2007; Zhang and Croy 2009).

High frequency ultrasound has been previously applied to the investigation of the uterine and umbilical arteries in the pregnant mouse throughout gestation (Khankin et al. 2012; MacLennan and Keller 1999; Phoon et al. 2000); however, besides from these two vessels, other fetal vascular territories have been scarcely evaluated. The aim of this study was to obtain Doppler recordings of fetal and placental vascular territories in CD-1 mice, similar to those obtained in the human fetus; in particular daily changes of the Doppler waveforms of the ductus venosus, which have not been described before; and to provide a better understanding of what is to be expected under normal circumstances in examining scarcely evaluated fetal vascular territories. This information is of interest to investigators studying the vascular adaptation/deterioration processes in experimental models of intrauterine growth restriction or preeclampsia.

Methods

Animals and Husbandry

The experiments described herein were conducted as part of an ongoing *in vivo* study for which the animal protocol approved by the Institutional Animal Care and Use Committee of Wayne State University, Detroit, MI, USA (IACUC protocol # A 11-03-11). Animal handling and care followed all the standards of the National Institutes of Health Guide for the Care and Use of Laboratory Animals: Eighth Edition (2011). (Washington, DC: The National Academies Press).

Thirteen pregnant CD-1 mice from Charles River Laboratories (Wilmington, MA, USA) were evaluated. Mice were kept in separate filtered-top rodent cages with *ad libitum* food

NIH-PA Author Manuscript

NIH-PA Author Manuscript

NIH-PA Author Manuscript

and water intake. Constant temperature (24±1°C) and humidity (50±5 %) were maintained in the animal room, with a daily regular 12:12 hour light-dark period.

Ultrasound recordings were performed daily from gestational day (GD) 8 to GD 18 in three mice; at GD 8, GD 13 and GD 18 in seven mice; and at GD 18 in three mice. The mice evaluated every day (n=3) constituted the group for which we studied daily hemodynamic changes; mice evaluated on GD 8, GD 13 and GD 18 (n=7) constituted the pilot group designed to optimize the main operative protocol; and the three mice evaluated on GD 18 formed the control group necessary to assess differences in neonatal characteristics among fetuses exposed to different periods of ultrasound insonation and anesthesia. No other experimental procedures were performed. A total of 26 fetuses (two per dam) were evaluated. Fifty seven scanning sessions were performed: 33 for the daily group, 21 for the group evaluated at GD 8, GD 13 and GD 18, and 3 for the control group.

Ultrasound assessments of maternal, fetal and placental blood flow

General anesthesia was induced by inhalation of 4–5% isoflurane (Aerrane; Baxter Healthcare Corporation, Deerfield, IL, USA) and 1L/minO_2. Anesthesia was maintained by inhalation with a mixture of 1–2% isoflurane and 1L/minO_2. Leakage of anesthesia gas was scavenged using a ventilation system equipped with a charcoal filter canister. Mice were positioned on a heating pad (Vevo Imaging Station, Visual Sonics Inc. Toronto, Ontario, Canada) and gently stabilized with adhesive tape (Figure 1). Abdominal and chest hair was shaved with a clipper, and was further cleaned with a chemical hair remover (Nair cream, Church & Dwight Canada Corp., Mississauga, Ontario, Canada) in order to minimize ultrasound attenuation. Nair cream was wiped off 15–20s after its application with alternating wet and dry gauzes to prevent damage to the skin. Mice cardiac and respiratory rates were registered during the entire ultrasound procedure and body temperature was maintained in the range of 37±1°C.

The first fetus in each uterine horn was evaluated with a high frequency linear 55 MHz ultrasound probe (Vevo 2010), Visual Sonics Inc. Toronto, Ontario, Canada). The ultrasound probe was fixed and mobilized with a mechanical holder. Fetal crown-rump length was first measured in all fetuses. The uterine arteries were located in the maternal pelvis on each side of the maternal bladder; the fetal carotid artery was visualized in a lateral sagittal view of the fetal thorax and neck; the fetal middle cerebral artery was localized in a cross sectional view of the fetal head at the level of the arterial circle; the ductus venosus was evaluated in a cross - sectional or sagittal view of the fetal abdomen before joining the inferior vena cava; and the umbilical artery and umbilical vein were visualized in an intra-amniotic segment of the umbilical cord, just after the cord exit from the fetal abdomen. (Figures 2 and 3). All Doppler recordings were performed at an angle of insonation as close as possible to 0°, and never greater than 45°. For maternal recordings, the velocity of the Doppler display was set at 0.8 cm/s, and for fetal recordings, at 2.6 cm/s. The size of the Doppler gate was kept between 0.3–0.5mm. Five to eight consecutive waveforms in each vessel in the absence of fetal movements, and without maternal respiratory movements were obtained. Peak systolic velocity (PSV) and end diastolic velocity (EDV) were calculated; additionally, atrial velocity (AV) in the ductus venosus was estimated. The resistance index

NIH-PA Author Manuscript

NIH-PA Author Manuscript

NIH-PA Author Manuscript

(RI) was calculated as: peak systolic velocity – end diastolic velocity / peak systolic velocity (Arbeille et al. 1983).

After ultrasound evaluation, and during the recovery period, mice were placed into their cages with one-half of each cage situated on a warm-water circulating blanket. All pups were delivered by cesarean on GD 18, and then weighed and measured. Newborn characteristics were compared between the groups of mice evaluated daily, mice evaluated on GD 8, GD 13 and GD 18 and mice evaluated only on GD 18. After cesarean, mice were euthanized in a CO_2 chamber according to the recommendation of the American Veterinary Medical Association (AVMA) Guidelines on Euthanasia.

Data and Statistical Analysis

Normality of the Doppler parameters distributions was assessed using the Kolmogorov-Smirnov test, inspection of histograms, and quantile-quantile (Q-Q) plots. Because multiple measurements within individual mice were correlated, generalized linear models for repeated measures were fit to assess the pattern of Doppler values over time using a robust covariance estimator. Transformations were performed where appropriate to meet parametric assumptions. Quadratic, cubic or quartic polynomials equations were selected to model these patterns over time to optimize model fit. Differences among groups were evaluated using one-way analysis of variance (ANOVA) with post hoc analysis. Chi square was used to estimate changes in the pulsatile pattern of the umbilical vein. A p value ≤ 0.05 was considered statistically significant. Statistical analyses were performed with Med Calc version 9.0.1.0 (Mariakerke, Belgium) and SAS version 9.3 (Carry, NC, USA) statistical analysis software.

Results

The complete ultrasound examination was performed on a median time of 37 minutes (range, 24–53 minutes). The uterine arteries were obtained in all animals during the period of examination. Doppler recordings of the umbilical artery and umbilical vein were obtained from GD 10, and from the middle cerebral artery, carotid artery and ductus venosus from GD 12. The relationship between gestational age with maternal weight, fetal heart rate and crown-rump length was best described using linear, quadratic and cubic functions, respectively (Figure 4).

Uterine arteries

(Figure 5.1a–c); A quadratic polynomials equation was used to model the relationships between peak systolic velocity and gestational age ($p=0.04$). End diastolic velocity increased linearly with gestational age ($p<0.001$) and the resistance index decreased linearly over time ($p=0.0004$).

Umbilical artery

(Figure 5.2a–c); The relationship between gestational age with mean peak systolic velocity and resistance index was best described using a quadratic polynomials equation Peak systolic velocity increased linearly from GD 11 to GD 17 ($p=0.0004$) and decreased at GD

NIH-PA Author Manuscript

NIH-PA Author Manuscript

NIH-PA Author Manuscript

18; end diastolic velocity was present from GD 15 and increased linearly over time ($p < 0.0001$). The resistance index was unchanged between GD 10 and GD 14, and decreased thereafter ($p=0.0001$).

Umbilical vein

Figure 2D shows the pulsatile pattern of the umbilical vein at GD 16 with 1 or 2 pulsations per second as compared with approximately 8 pulsations per second at GD 14 (image not shown) ($p<0.05$).

Carotid

(Figure 6.1a–c) and middle cerebral arteries (Figure 6.2a–c): While peak systolic velocity increased linearly with gestational age ($p<0.001$) in the carotid artery, a quadratic relationship was observed in the middle cerebral artery ($p=0.02$). In both the carotid and middle cerebral arteries, a quadratic curve best described the relationship between end diastolic velocity and gestational age (both $p<0.0001$); an inverse quadratic curve best described the relationship between resistance index and gestational age in both arteries (both $p<0.0001$).

Ductus Venosus

The ductus venosus waveform showed characteristics similar to human fetuses (Figure 3). There was a clearly visible bright color spot in its narrow portion before the junction with the inferior vena cava. The Doppler waveform presented three components: systolic, diastolic and atrial. Quadratic polynomials equation best described the relationship between the three velocities and the resistance index with gestational age in this vessel (peak systolic velocity, $p=0.02$; end diastolic velocity, $p=0.01$; atrial velocity, $p<0.0001$, resistance index $p=0.01$) (Figure 7).

Discussion

The principal findings of this study are: 1) consistent evaluation of fetal and maternal vascular Doppler velocities in CD-1 mice is possible using high frequency ultrasound; 2) Doppler waveforms of the fetal and maternal vessels were similar to those observed in human pregnancy; 3) increased diastolic velocities and reduced resistance index in all fetal vascular territories toward the end of pregnancy, 4) the ductus venosus waveform was consistently obtained after GD 12.

The increase in Doppler velocities and reduction of the resistance index toward the end of pregnancy might represent the continuous development of fetal organ vascular networks. Development of the cardiovascular system in the fetal mouse, starting at GD 7.5 is characterized by a process of vascular proliferation, sprouting and pruning, which creates a complex network of branched endothelial tubes of different diameters that reduce the resistance to blood flow (Drake and Fleming 2000; Isogai et al. 2003; Walls et al. 2008). Simultaneously, the development of the fetal heart begins at GD 7 (Ji et al. 2003); by GD 8 the primitive heart consists of a pulsatile tube; by GD 9.5 a common atrial chamber and a primitive ventricle are observed (Srinivasan et al. 1998). From GD 10 the fetal heart passes

NIH-PA Author Manuscript

NIH-PA Author Manuscript

NIH-PA Author Manuscript

through a sequence of anatomical changes and rotations until GD 15, when it reaches its definitive shape and anatomy (Keller et al. 1996; Srinivasan et al. 1998). During this period the heart rate increases from 120 to 190 beats per minute (Keller et al. 1996). Our findings show a similar increment in the fetal heart rate, a stable pattern in the waveform velocities, and a decrease in the resistance index from GD 16 onward, consistent with the period when the heart and the vascular system attain functional maturation (Lucitti et al. 2007).

Ultrasound evaluation of fetal mice has been previously reported using either conventional or high-frequency ultrasound. Brown et al. (2006) used a 15 MHz probe and conventional ultrasound equipment to count the number of fetuses and to estimate the crown-rump length, from GD 9.5 until the end of pregnancy using a freehand technique. Even with success in obtaining these basic estimations, neither detailed anatomy nor hemodynamic data were described. The authors acknowledged that it was not possible to obtain detailed information about fetal, placental and maternal structures using conventional ultrasound. Mu & Adamson (2006) used high-frequency ultrasound for daily evaluation of the uterine and umbilical arteries from GD 6 to GD 18. Similar to our results, they showed a progressive increase in systolic and diastolic velocities, and a reduction in the resistance index of both vessels throughout gestation. The authors suggested that the increase in the umbilical artery diastolic flow might be related to the final process of fetal organogenesis. We also consider that can also be related to a lower placental resistance to blood flow. Khankin et al. (2012) also evaluated the uterine and umbilical arteries at GD 13 and GD 18 and showed, similar to our results, an increase in systolic and diastolic velocities in both blood vessels; however, no significant reduction in the umbilical artery resistance index was noted. The two mentioned articles reported changes only for the uterine and/or umbilical arteries; in the present study we also included the examination of the carotid and cerebral arteries, and the evaluation of the ductus venosus, thus offering a more complete perspective of arterial and venous hemodynamic changes of the fetal mouse throughout pregnancy. The increased diastolic velocities in the carotid and cranial arteries towards the end of pregnancy suggested an increment in the intracranial blood flow in late periods of gestation. Similarly, the ductus venosus showed a progressive increase in diastolic and atrial blood velocities, probably due to more oxygenated blood in the umbilical vein. This is the first report showing simultaneous evaluation of all these vascular parameters.

The technique for obtaining Doppler recordings in the common carotid and middle cerebral arteries in fetal mice was previously described by Bake et al. (2012). They reported changes in these vessels when pregnant mice were exposed to alcohol. We acquired Doppler recordings using a similar approach. Although the carotid artery was relatively easy to obtain, the anatomical projection and angle of insonation limited the interpretation of true velocity. Waveforms from the middle cerebral artery were obtained in a cross-sectional view of the fetal head, similar to that used in human fetuses, providing a good insonation angle and reliable velocity estimations. In the carotid and middle cerebral arteries, end diastolic velocity appeared from GD 12 onward. The two vessels showed a similar trend of increasing velocities and reduced resistance index toward the end of pregnancy. Doppler investigation of the ductus venosus showed a triphasic component, similar to that observed in human fetuses, consisting in a systolic peak, diastolic peak and positive atrial peak. The ductus venosus was identified by following the intra-abdominal trajectory of the umbilical vein and

NIH-PA Author Manuscript

NIH-PA Author Manuscript

NIH-PA Author Manuscript

the detection of aliasing produced by increased blood velocity in its narrow region. Previously, Dickinson et al.(2008) studied the ductus venosus in a different genus known as the *spiny mouse*. This genus has a longer gestational period (38 days) and bears fewer and larger fetuses than CD-1 mice. Fetal mice also showed a triphasic waveform and an increase in velocities throughout the end of pregnancy with no changes in the resistance index. No previous reports on the daily changes of the ductus venous velocity waveform in CD-1 mice, or in similar mouse species were found in the literature

Technical considerations

Although some authors have used a freehand acquisition of ultrasound images (Brown et al. 2006), the platform and mechanical holder of the ultrasound probe proved to be of major importance for obtaining good quality Doppler waveforms. Small movements can change the angle of insonation, giving erroneous assessment of the Doppler velocities. Despite the limited mobility of the mechanical holder, only two anatomical views were necessary to obtain all hemodynamic estimations: 1) a cross-sectional view of the fetus, where the ultrasound probe was swiped from head to tail, provided images of almost all anatomical organs and adequate insonantion angles of the umbilical artery, umbilical vein, middle cerebral artery, and ductus venosus; and 2), by rotating the ultrasound transducer by 90°, a sagittal plane was obtained for the measurement of the crown-rump length. Additionally, in the latter, by swiping the ultrasound probe form left to right, recordings of the carotid arteries, umbilical artery, umbilical vein, and ductus venosus were obtained.

Doppler recordings were affected by fetal body movements and maternal breathing. Although fetal mouse movements are not very common, tiny movements can change the anatomical section used for examination. Maternal respiratory movements might also affect the quality of the recordings; fortunately, the high maternal and fetal heart rate allowed clear recordings of at least three to four waveforms between respiratory movements.

Time exposure and anesthesia

The effect of anesthesia on the hemodynamic parameters in the fetal mouse is not known. To reduce exposure to anesthesia, Jaiswal et al. (2009) proposed immobilizing the mouse in a ventral position without sedation. This approach was used for the evaluation of the ovaries in which insonation was performed from the back of the mouse. However, for abdominal examination, the mouse needs to lie on its back. In this position, the mouse cannot be safely immobilized without sedation. We kept exposure to anesthesia to a maximum of one hour; in the majority of sessions, the study was completed in less than 40 minutes. We did not find differences in birth weight, neonatal measurements, and placental weight and size among fetuses exposed to anesthesia and high-frequency ultrasound daily, three times during pregnancy or only before delivery.

Clinical implications

Mice and humans have placentas with similar anatomical and functional characteristics (Carter 2007; Georgiades et al. 2002). Both have discoid placentas with a common phylogenetic origin and similar functional units (labyrinth in the mouse, and villous tree in humans) (Wildman et al. 2006). Cox et al. reported that more than 70% of genes involved in

NIH-PA Author Manuscript

NIH-PA Author Manuscript

NIH-PA Author Manuscript

nutrient transport are co-expressed in human and mouse placentas (2009). This makes the pregnant mouse an interesting and convenient model for studying severe and frequent perinatal complications related to placental dysfunction such as preeclampsia and intrauterine growth restriction (Watson and Cross 2005). High frequency ultrasound might provide important information about the fetal cardiovascular response when these complications develop.

Conclusion

Using high-frequency ultrasound, evaluation of maternal and fetal Doppler parameters in pregnant mice, similar to those obtained during human fetal surveillance, can be completed in about 40 minutes with short exposure to anesthesia. Hemodynamic changes in experimentally-induced pathologic conditions (preeclampsia, intrauterine growth restriction, diabetes) or in knock-out mouse models can be studied using high-frequency ultrasound. These results can be compared to those obtained from human fetuses in order to evaluate the process of adaptation or deterioration related to obstetrical complications.

Acknowledgments

This research was supported, in part, by the Perinatology Research Branch, Division of Intramural Research, *Eunice Kennedy Shriver* National Institute of Child Health and Human Development, National Institutes of Health, Department of Health and Human Services (NICHD/NIH); and, in part, with Federal funds from NICHD, NIH under Contract No. HHSN275201300006C.

The authors are grateful to Dr. Lisa Brossia, DVM, MS, Laura McIntyre, LVT and all personnel at the Division of Laboratory Animal Resources of Wayne State University who provided veterinary care and husbandry for the animals used in this study. We are grateful to Maureen McGerty and Andrea Bernard (Wayne State University) for editorial support. The authors wish to dedicate this work to the memory of our colleague Mary King RDMS who was part of our team for more than a decade.

References

Abi-Nader KN, Boyd M, Flake AW, Mehta V, Peebles D, David AL. Animal models for prenatal gene therapy: the sheep model. Methods in molecular biology. 2012; 891:219–248. [PubMed: 22648775]

Acharya G, Rasanen J, Makikallio K, Erkinaro T, Kavasmaa T, Haapsamo M, Mertens L, Huhta JC. Metabolic acidosis decreases fetal myocardial isovolumic velocities in a chronic sheep model of increased placental vascular resistance. Am J Physiol Heart Circ Physiol. 2008; 294:H498–H504. [PubMed: 18024549]

Arbeille P, Asquier E, Moxhon E, Magnin M, Pourcelot L, Berger C, Lansac J. Study of fetal and placental circulation by ultrasound. New technic in the surveillance of pregnancy. J Gynecol Obstet Biol Reprod (Paris). 1983; 12:851–859. [PubMed: 6672078]

Bake S, Tingling JD, Miranda RC. Ethanol exposure during pregnancy persistently attenuates cranially directed blood flow in the developing fetus: evidence from ultrasound imaging in a murine second trimester equivalent model. Alcohol Clin Exp Res. 2012; 36:748–758. [PubMed: 22141380]

Bassan H, Trejo LL, Kariv N, Bassan M, Berger E, Fattal A, Gozes I, Harel S. Experimental intrauterine growth retardation alters renal development. Pediatric nephrology. 2000; 15:192–195. [PubMed: 11149109]

Bennet L, Rossenrode S, Gunning MI, Gluckman PD, Gunn AJ. The cardiovascular and cerebrovascular responses of the immature fetal sheep to acute umbilical cord occlusion. J Physiol. 1999; 517(Pt 1):247–257. [PubMed: 10226163]

Berman W Jr, Goodlin RC, Heymann MA, Rudolph AM. Measurement of umbilical blood flow in fetal lambs in utero. J Appl Physiol. 1975; 39:1056–1059. [PubMed: 1213965]

NIH-PA Author Manuscript

NIH-PA Author Manuscript

NIH-PA Author Manuscript

Bishai JM, Blood AB, Hunter CJ, Longo LD, Power GG. Fetal lamb cerebral blood flow (CBF) and oxygen tensions during hypoxia: a comparison of laser Doppler and microsphere measurements of CBF. J Physiol. 2003; 546:869–878. [PubMed: 12563011]

Block BS, Llanos AJ, Creasy RK. Responses of the growth-retarded fetus to acute hypoxemia. Am J Obstet Gynecol. 1984; 148:878–885. [PubMed: 6711629]

Brown SD, Zurakowski D, Rodriguez DP, Dunning PS, Hurley RJ, Taylor GA. Ultrasound diagnosis of mouse pregnancy and gestational staging. Comp Med. 2006; 56:262–271. [PubMed: 16941953]

Carter AM. Animal models of human placentation--a review. Placenta. 2007; 28(Suppl A):S41–S47. [PubMed: 17196252]

Cox B, Kotlyar M, Evangelou AI, Ignatchenko V, Ignatchenko A, Whiteley K, Jurisica I, Adamson SL, Rossant J, Kislinger T. Comparative systems biology of human and mouse as a tool to guide the modeling of human placental pathology. Mol Syst Biol. 2009; 5:279. [PubMed: 19536202]

Dickinson H, Griffiths T, Walker DW, Jenkin G. Application of clinical indices of fetal growth and wellbeing to a novel laboratory species, the spiny mouse. Reprod Biol. 2008; 8:229–243. [PubMed: 19092985]

Drake CJ, Fleming PA. Vasculogenesis in the day 6.5 to 9.5 mouse embryo. Blood. 2000; 95:1671–1679. [PubMed: 10688823]

Eixarch E, Figueras F, Hernandez-Andrade E, Crispi F, Nadal A, Torre I, Oliveira S, Gratacos E. An experimental model of fetal growth restriction based on selective ligature of uteroplacental vessels in the pregnant rabbit. Fetal Diagn Ther. 2009; 26:203–211. [PubMed: 19955698]

Eixarch E, Hernandez-Andrade E, Crispi F, Illa M, Torre I, Figueras F, Gratacos E. Impact on fetal mortality and cardiovascular Doppler of selective ligature of uteroplacental vessels compared with undernutrition in a rabbit model of intrauterine growth restriction. Placenta. 2011; 32:304–309. [PubMed: 21334065]

Ferrazzi E, Bellotti M, Galan H, Pennati G, Bozzo M, Rigano S, Battaglia FC. Doppler investigation in intrauterine growth restriction--from qualitative indices to flow measurements: a review of the experience of a collaborative group. Ann N Y Acad Sci. 2001; 943:316–325. [PubMed: 11594551]

Georgiades P, Ferguson-Smith AC, Burton GJ. Comparative developmental anatomy of the murine and human definitive placentae. Placenta. 2002; 23:3–19. [PubMed: 11869088]

Gudmundsson S, Eik-Nes S, Lingman G, Vernersson E, Grip A, Kristofferson K, Marsal K. Evaluation of blood flow velocity waveform in an animal model. Echocardiography. 1990; 7:647–656. [PubMed: 10150002]

Gunnarsson GO, Gudmundsson S, Hokegard K, Stale H, Kjellmer I, Hafstrom O, Marsal K. Cerebral Doppler blood flow velocimetry and central hemodynamics in the ovine fetus during hypoxemia-acidemia. J Perinat Med. 1998; 26:107–114. [PubMed: 9650131]

Hernandez-Andrade E, Hellstrom-Westas L, Thorngren-Jerneck K, Jansson T, Liuba K, Lingman G, Marsal K, Oskarsson G, Werner O, Ley D. Perinatal adaptive response of the adrenal and carotid blood flow in sheep fetuses subjected to total cord occlusion. J Matern Fetal Neonatal Med. 2005; 17:101–109. [PubMed: 16076616]

Heymann MA, Payne BD, Hoffman JI, Rudolph AM. Blood flow measurements with radionuclide-labeled particles. Prog Cardiovasc Dis. 1977; 20:55–79. [PubMed: 877305]

Heymann MA, Rudolph AM. Effect of exteriorization of the sheep fetus on its cardiovascular function. Circ Res. 1967; 21:741–745. [PubMed: 5624122]

Isogai S, Lawson ND, Torrealday S, Horiguchi M, Weinstein BM. Angiogenic network formation in the developing vertebrate trunk. Development. 2003; 130:5281–5290. [PubMed: 12954720]

Jaiswal RS, Singh J, Adams GP. High-resolution ultrasound biomicroscopy for monitoring ovarian structures in mice. Reprod Biol Endocrinol. 2009; 7:69. [PubMed: 19580664]

Ji RP, Phoon CK, Aristizabal O, McGrath KE, Palis J, Turnbull DH. Onset of cardiac function during early mouse embryogenesis coincides with entry of primitive erythroblasts into the embryo proper. Circ Res. 2003; 92:133–135. [PubMed: 12574139]

Keller BB, MacLennan MJ, Tinney JP, Yoshigi M. In vivo assessment of embryonic cardiovascular dimensions and function in day-10.5 to -14.5 mouse embryos. Circ Res. 1996; 79:247–255. [PubMed: 8756001]

NIH-PA Author Manuscript

NIH-PA Author Manuscript

NIH-PA Author Manuscript

Khankin EV, Hacker MR, Zelop CM, Karumanchi SA, Rana S. Intravital high-frequency ultrasonography to evaluate cardiovascular and uteroplacental blood flow in mouse pregnancy. Pregnancy Hypertens. 2012; 2:84–92. [PubMed: 22544045]

Lucitti JL, Jones EA, Huang C, Chen J, Fraser SE, Dickinson ME. Vascular remodeling of the mouse yolk sac requires hemodynamic force. Development. 2007; 134:3317–3326. [PubMed: 17720695]

MacLennan MJ, Keller BB. Umbilical arterial blood flow in the mouse embryo during development and following acutely increased heart rate. Ultrasound Med Biol. 1999; 25:361–370. [PubMed: 10374980]

Malassine A, Frendo JL, Evain-Brion D. A comparison of placental development and endocrine functions between the human and mouse model. Hum Reprod Update. 2003; 9:531–539. [PubMed: 14714590]

Mu J, Adamson SL. Developmental changes in hemodynamics of uterine artery, utero- and umbilicoplacental, and vitelline circulations in mouse throughout gestation. Am J Physiol Heart Circ Physiol. 2006; 291:H1421–H1428. [PubMed: 16603699]

Pham V, Burns P, Albiston AL, Yeatman HR, Ng L, Diwakarla S, Chai SY. Reproduction and maternal behavior in insulin-regulated aminopeptidase (IRAP) knockout mice. Peptides. 2009; 30:1861–1865. [PubMed: 19647771]

Phoon CK, Aristizabal O, Turnbull DH. 40 MHz Doppler characterization of umbilical and dorsal aortic blood flow in the early mouse embryo. Ultrasound Med Biol. 2000; 26:1275–1283. [PubMed: 11120365]

Renault G, Bonnin P, Marchiol-Fournigault C, Gregoire JM, Serriere S, Richard B, Fradelizi D. High-resolution ultrasound imaging of the mouse. J Radiol. 2006; 87:1937–1945. [PubMed: 17211308]

Rosen KG, Hrbek A, Karlsson K, Kjellmer I. Fetal cerebral, cardiovascular and metabolic reactions to intermittent occlusion of ovine maternal placental blood flow. Acta physiologica Scandinavica. 1986; 126:209–216. [PubMed: 3705984]

Rudolph AM, Heymann MA. The circulation of the fetus in utero. Methods for studying distribution of blood flow, cardiac output and organ blood flow. Circ Res. 1967; 21:163–184. [PubMed: 4952708]

Rudolph AM, Heymann MA. The fetal circulation. Annu Rev Med. 1968; 19:195–206. [PubMed: 4871686]

Rudolph AM, Heymann MA. Circulatory changes during growth in the fetal lamb. Circ Res. 1970; 26:289–299. [PubMed: 5461210]

Rudolph AM, Heymann MA. Measurement of flow in perfused organs, using microsphere techniques. Acta Endocrinol Suppl (Copenh). 1972; 158:112–127. [PubMed: 4536841]

Sapin V, Blanchon L, Serre AF, Lemery D, Dastugue B, Ward SJ. Use of transgenic mice model for understanding the placentation: towards clinical applications in human obstetrical pathologies? Transgenic Res. 2001; 10:377–398. [PubMed: 11708649]

Schmidt KG, Di Tommaso M, Silverman NH, Rudolph AM. Evaluation of changes in umbilical blood flow in the fetal lamb by Doppler waveform analysis. Am J Obstet Gynecol. 1991; 164:1118–1126. [PubMed: 2014838]

Sheldon RE, Peeters LL, Jones MD Jr, Makowski EL, Meschia G. Redistribution of cardiac output and oxygen delivery in the hypoxemic fetal lamb. Am J Obstet Gynecol. 1979; 135:1071–1078. [PubMed: 517592]

Smith SE, Li J, Garbett K, Mirnics K, Patterson PH. Maternal immune activation alters fetal brain development through interleukin-6. J Neurosci. 2007; 27:10695–10702. [PubMed: 17913903]

Srinivasan S, Baldwin HS, Aristizabal O, Kwee L, Labow M, Artman M, Turnbull DH. Noninvasive, in utero imaging of mouse embryonic heart development with 40-MHz echocardiography. Circulation. 1998; 98:912–918. [PubMed: 9738647]

Stypmann J. Doppler ultrasound in mice. Echocardiography. 2007; 24:97–112. [PubMed: 17214632]

Tian Y, Jackson P, Gunter C, Wang J, Rock CO, Jackowski S. Placental thrombosis and spontaneous fetal death in mice deficient in ethanolamine kinase 2. J Biol Chem. 2006; 281:28438–28449. [PubMed: 16861741]

Walls JR, Coultas L, Rossant J, Henkelman RM. Three-dimensional analysis of vascular development in the mouse embryo. PLoS One. 2008; 3:e2853. [PubMed: 18682734]

NIH-PA Author Manuscript

NIH-PA Author Manuscript

NIH-PA Author Manuscript

Watson ED, Cross JC. Development of structures and transport functions in the mouse placenta. Physiology (Bethesda). 2005; 20:180–193. [PubMed: 15888575]

Wildman DE, Chen C, Erez O, Grossman LI, Goodman M, Romero R. Evolution of the mammalian placenta revealed by phylogenetic analysis. Proc Natl Acad Sci U S A. 2006; 103:3203–3208. [PubMed: 16492730]

Zhang J, Adams MA, Croy BA. Alterations in maternal and fetal heart functions accompany failed spiral arterial remodeling in pregnant mice. Am J Obstet Gynecol. 2011; 205:485, e1–e16. [PubMed: 21831352]

Zhang J, Croy BA. Using ultrasonography to define fetal-maternal relationships: moving from humans to mice. Comp Med. 2009; 59:527–533. [PubMed: 20034427]

NIH-PA Author Manuscript
NIH-PA Author Manuscript
NIH-PA Author Manuscript

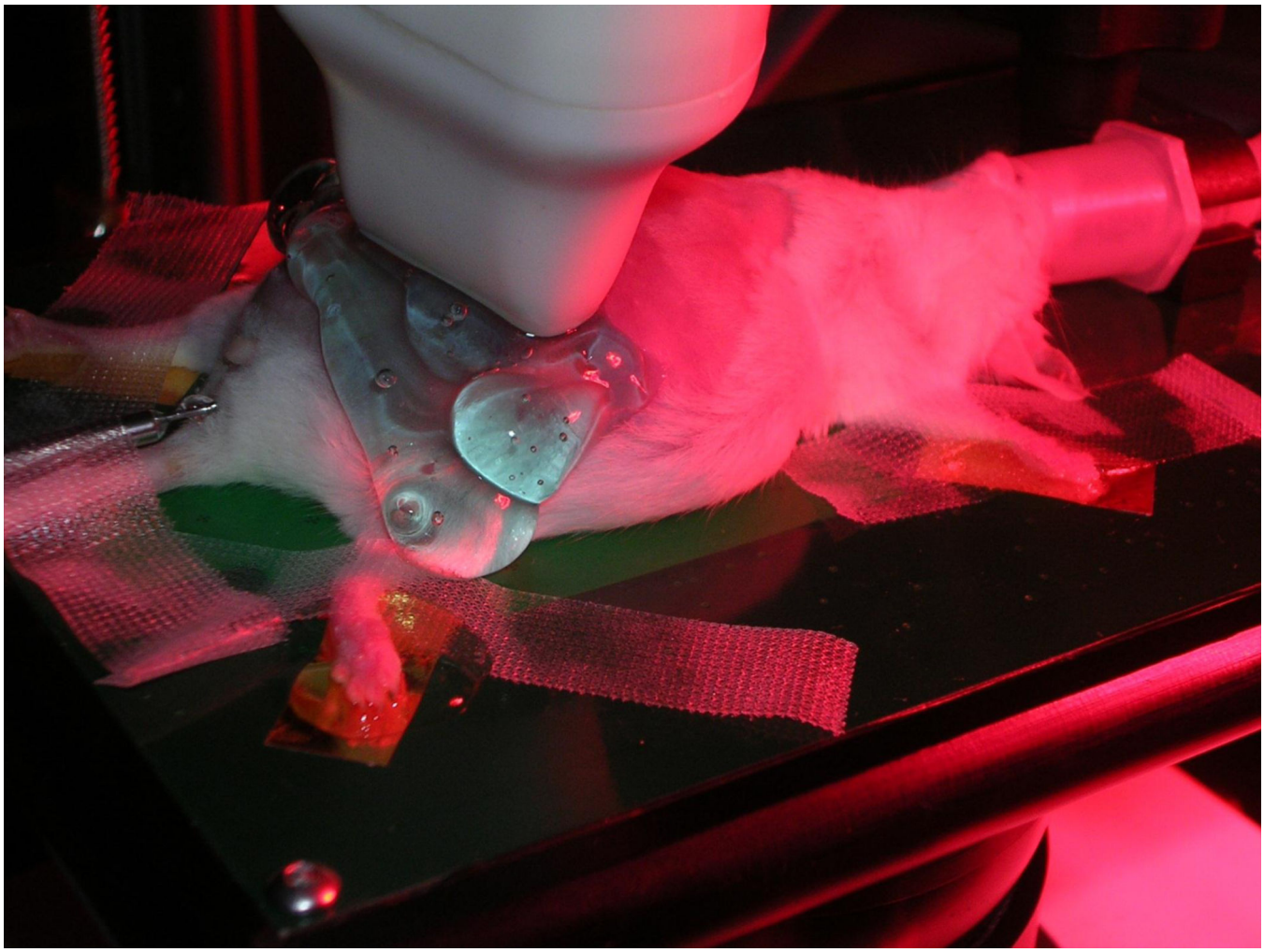

Figure 1.
Position of a pregnant mouse in the ultrasound scanning platform

NIH-PA Author Manuscript
NIH-PA Author Manuscript
NIH-PA Author Manuscript

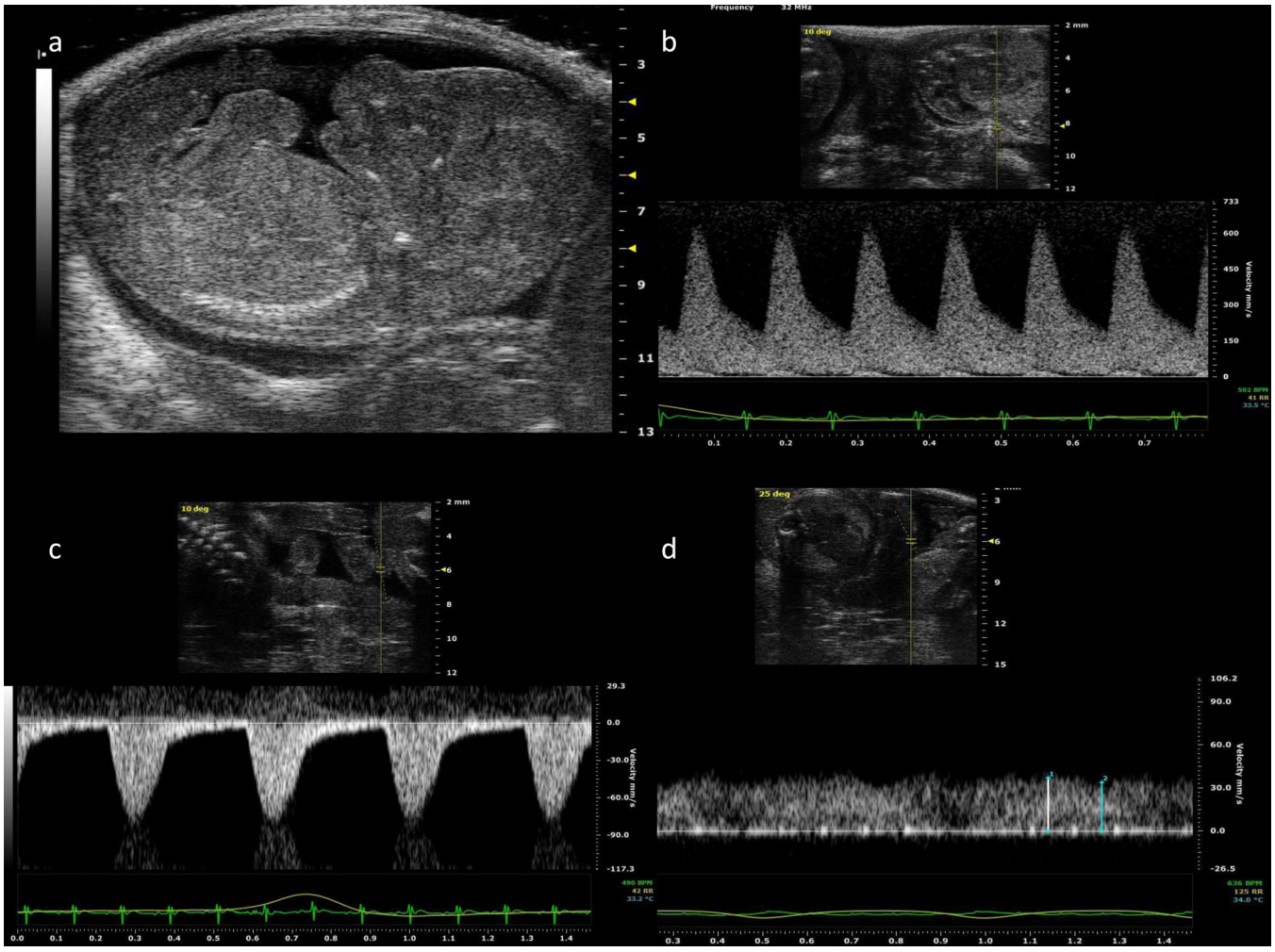

Figure 2.

a) Midsagittal view of a fetal mouse at gestational day 17; b) Doppler waveforms of the uterine artery, c) umbilical artery, and d) umbilical vein at gestational day 16.

NIH-PA Author Manuscript
NIH-PA Author Manuscript
NIH-PA Author Manuscript

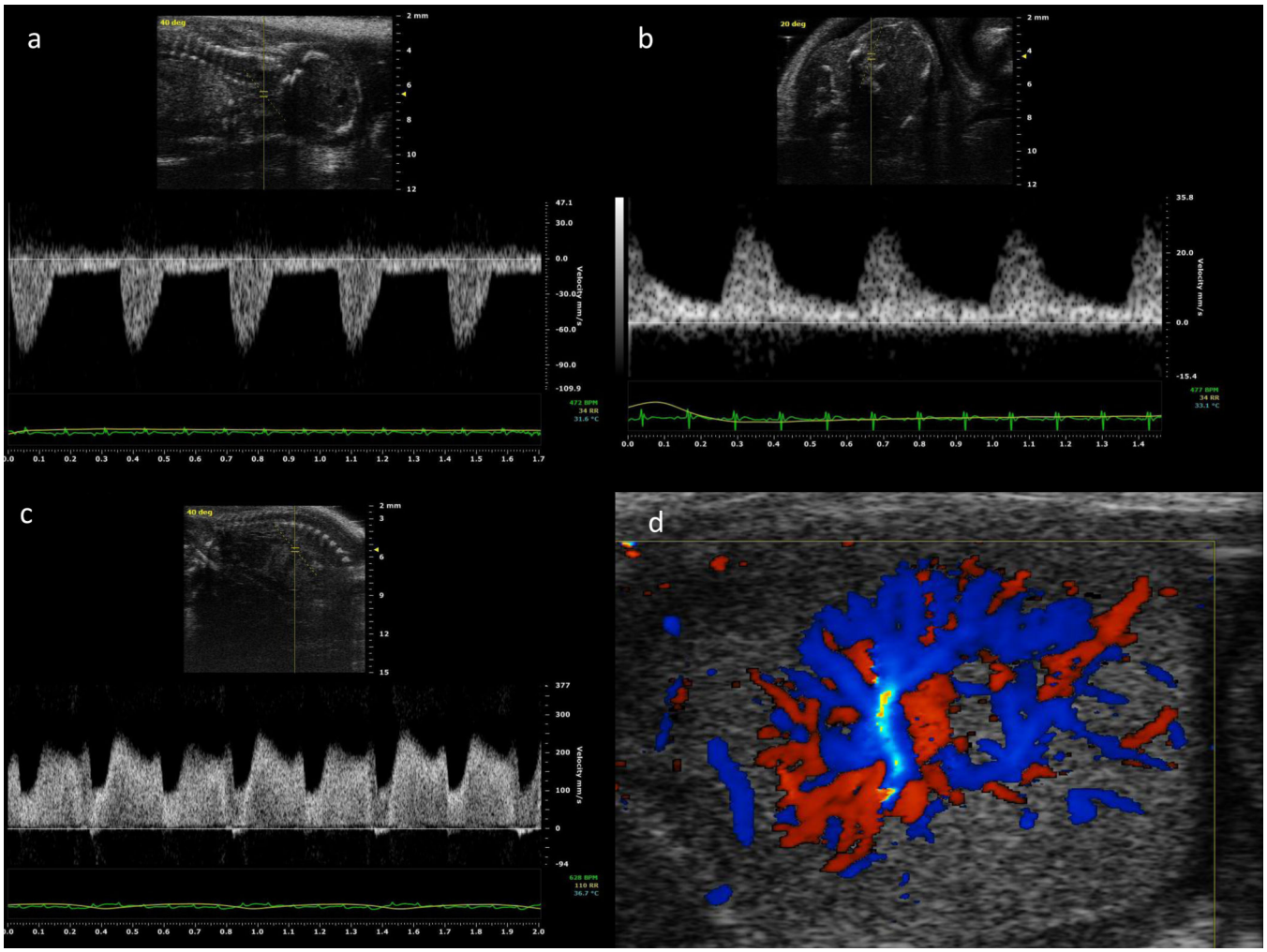

Figure 3.

Doppler waveforms of: a) common carotid artery; b) middle cerebral artery; c) ductus venosus; and d) color Doppler velocimetry of intraplacental vessels at gestational day 16.

NIH-PA Author Manuscript
NIH-PA Author Manuscript
NIH-PA Author Manuscript

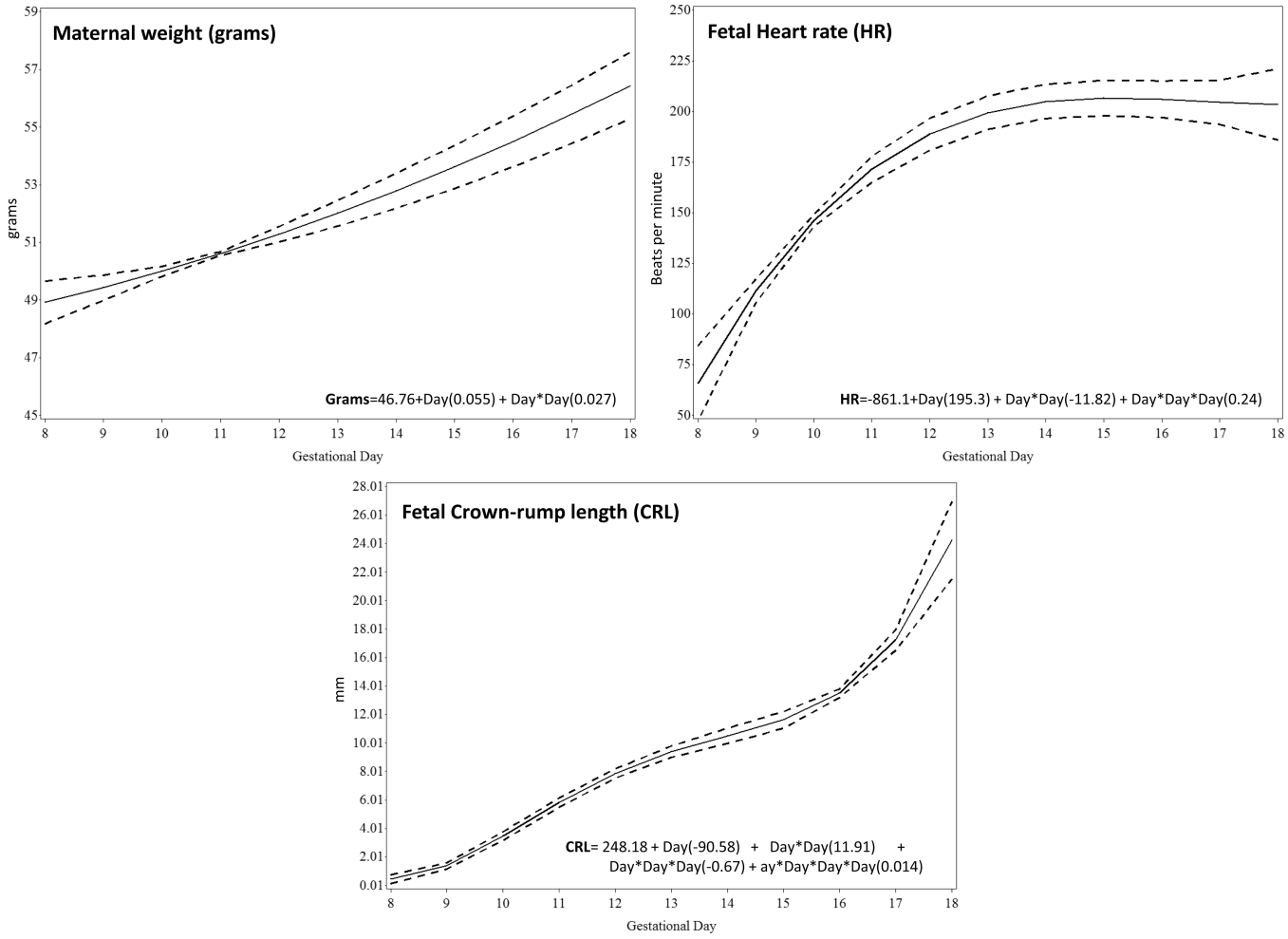

Figure 4.

Changes during gestation of maternal weight (a), fetal heart rate (FHR) (b), and fetal crown-rump length (CRL) (c). The solid line represents the best fitting mean determined using a generalized linear model, whereas dashed lines represent the 95% confidence limits of the mean.

NIH-PA Author Manuscript
NIH-PA Author Manuscript
NIH-PA Author Manuscript

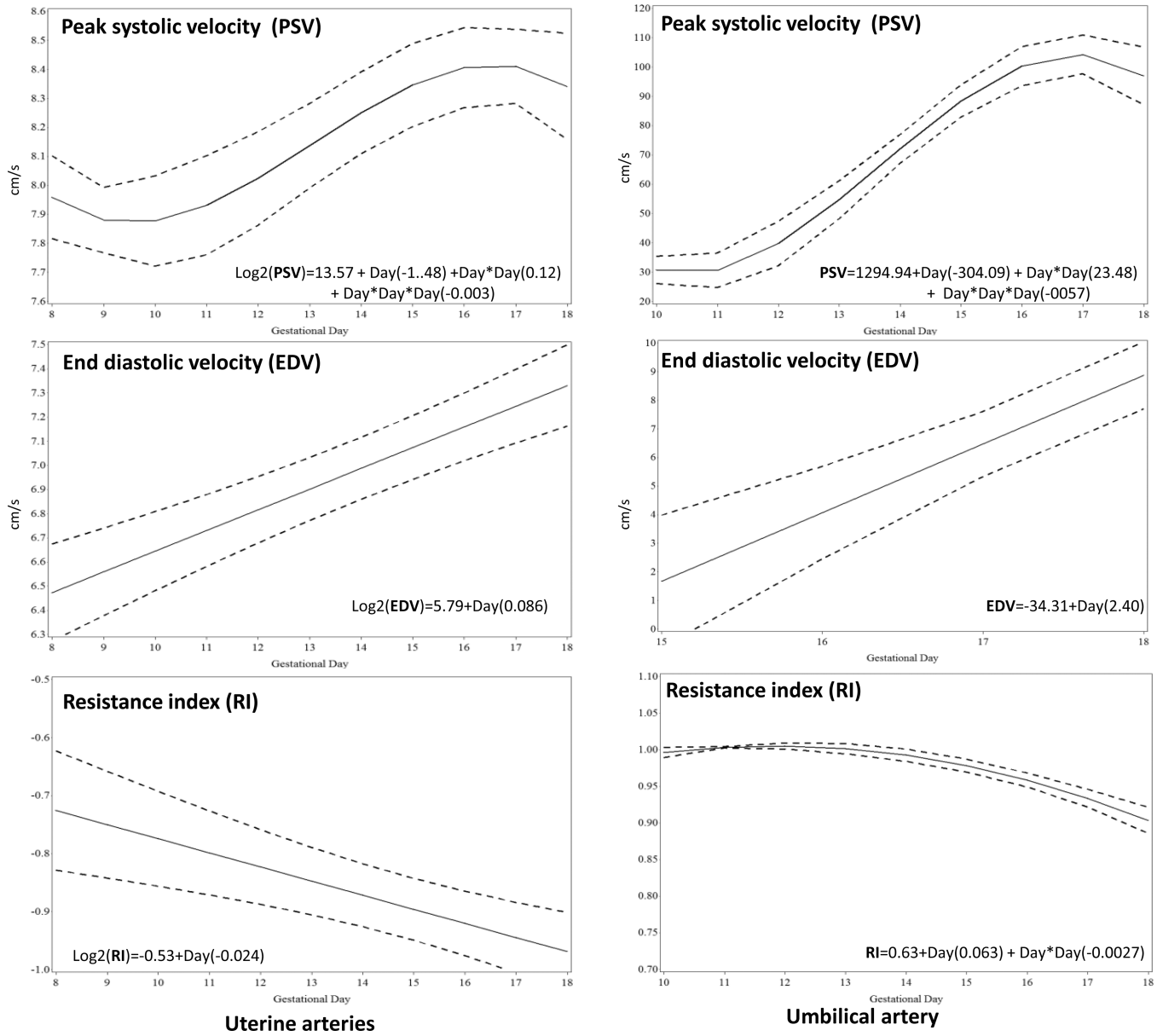

Figure 5.

Doppler velocities and resistance index (RI) during gestation of the uterine artery PSV, peak systolic velocity (1a); EDV, end diastolic velocity (1b); RI, resistance index (1c) and umbilical artery PSV, peak systolic velocity (2a); EDV, end diastolic velocity (2b); RI, resistance index (2c). The solid line represents the best fitting mean determined using a generalized linear model, whereas dashed lines represent the 95% confidence limits of the mean.

NIH-PA Author Manuscript
NIH-PA Author Manuscript
NIH-PA Author Manuscript

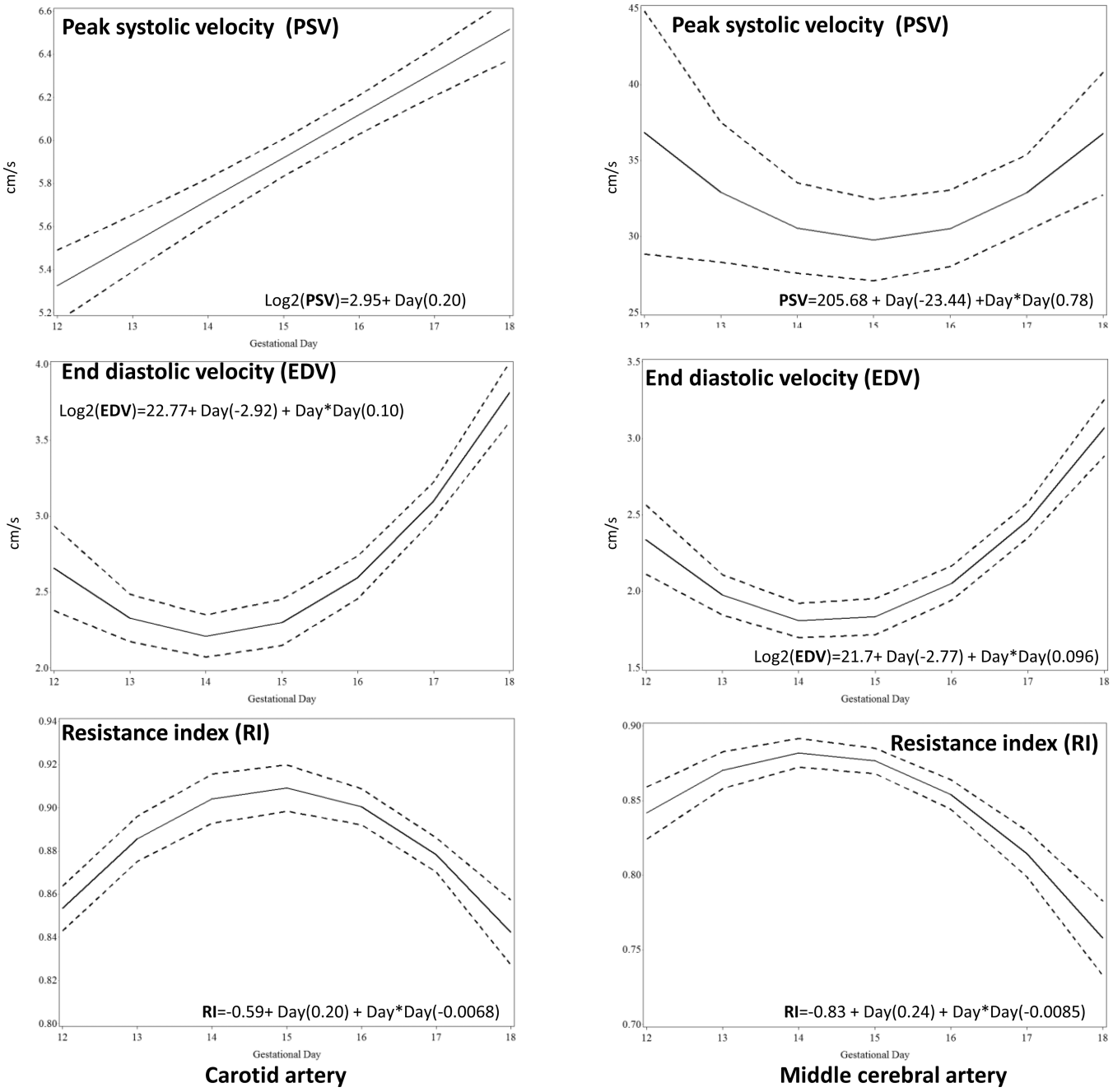

Figure 6.

Doppler velocities and resistance index (RI) from gestational day 12 to gestational day 18 of the common carotid artery PSV, peak systolic velocity (1a); EDV, end diastolic velocity (1b); RI, resistance index (1c) and middle cerebral artery PSV, peak systolic velocity (2a); EDV, end diastolic velocity (2b); RI, resistance index (2c). The solid line represents the best fitting mean determined using a generalized linear model, whereas dashed lines represent the 95% confidence limits of the mean.

NIH-PA Author Manuscript
NIH-PA Author Manuscript
NIH-PA Author Manuscript

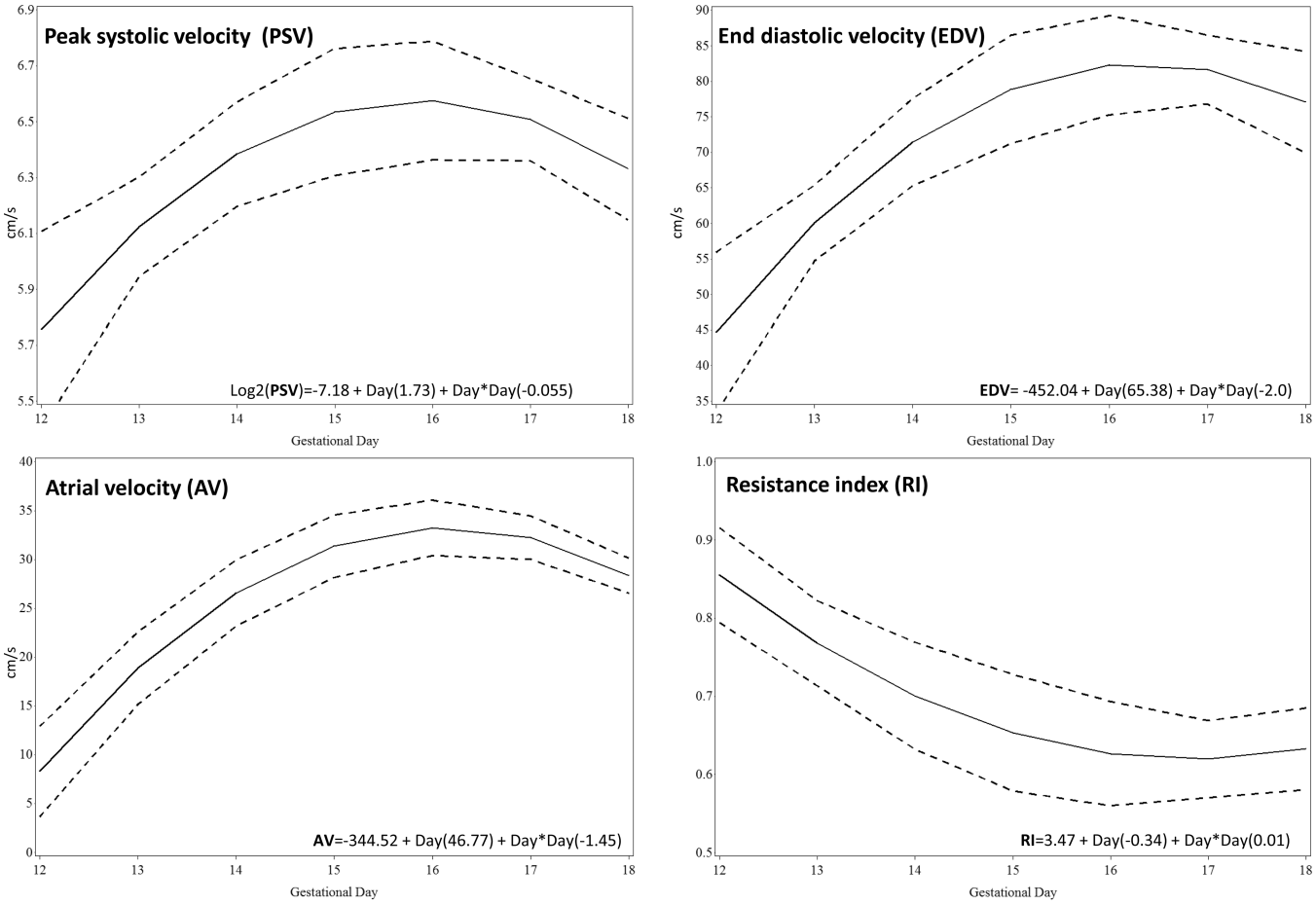

Figure 7.

Doppler velocities and resistance index (RI) from gestational day 12 to gestational day 18 of the ductus venosus. The solid line represents the best fitting mean determined using a generalized linear model, whereas dashed lines represent the 95% confidence limits of the mean. PSV, peak systolic velocity; EDV, end diastolic velocity; RI, resistance index; AF, atrial flow.

NIH-PA Author Manuscript
NIH-PA Author Manuscript
NIH-PA Author Manuscript

Table 1

Characteristics of newborn mice

	Mice evaluated from GD 8 to GD 18 (Pregnant dams n=3, fetuses n= 6)	Mice evaluated at GD 8, GD13 and GD18 (Pregnant dams n=7, fetuses n=14)	Mice evaluated at GD 18 (Pregnant dams n=3, fetuses n=6)	p Value
Birthweight (grams [median, range])	1.05 (0.97–1.22)	1.02 (0.96–1.19)	1.05 (0.01–1.24)	0.64
Neonatal length (mm [median, range])	22.0 (16.8–25.6)	19.15 (16.8–22.69)	21.02 (16.4–24.3)	0.11
Biparietal diameter (mm [median, range])	6.29 (5.99–6.78)	6.17 (5.84–6.68)	6.19 (5.92–6.75)	0.21
Placental weight (grams [median, range])	0.12 (0.08–0.18)	0.11 (0.07–0.19)	0.12 (0.08–0.17)	0.85
Placental diameter (mm [median, range])	8.19 (6.28–9.72)	8.06 (6.0–9.42)	8.14 (6.0–9.65)	0.45